Synthesis and Reactivity of Dithienopyrazines

Franziska Kreuzer,[a,b] Elena Mena-Osteritz,[a] Peter Bäuerle*[a]

[a] Institute of Organic Chemistry II and Advanced Materials, University of Ulm, Albert-Einstein-Allee 11, 89081 Ulm, Germany; [b] Mattson Thermal Products GmbH, 89160 Dornstadt, Germany

Abstract: Heteroacenes developed to widely used building blocks in organic semiconductors for application in organic electronics due to their tunable structures and properties concomitant with inherent stability. Here, we report efficient preparation and investigation of so far unknown heterotriacenes, basic *anti*- and *syn*-dithienopyrazines **5** and **6**. The comparison of the two isomers with respect to electronic properties and follow-up reactions gives insights into structure-property and -reactivity relationships. Examples of transition metal-catalyzed C-C cross-coupling reactions of corresponding halogenated derivatives show the practical impact for extended π-conjugated systems applied in optoelectronic devices.

Introduction

The chemical structure of organic molecules and materials, which are applied in organic electronic devices such as organic light emitting diodes, solar cells, or batteries, determines their performance to a great extent.[1] Therefore, structure-property relationships are a vital basis for the optimal design of organic semiconductors. In this respect, there is a great interest in the development of novel π-conjugated polycyclic molecules such as acenes,[2] phenacenes,[3] or nanographenes.[4] Corresponding heteroacenes, which contain heteroatoms such as nitrogen or sulfur represent encouraging alternatives to the pure hydrocarbons, because electronic properties are tunable and chemical stability is typically increased.[5,6]

One of the most prominent example is represented by benzo[1,2-*b*:4,5-*b'*]dithiophene **1**, which was very successfully implemented as synthon in a multitude of oligomeric[7] and polymeric materials[8] for efficient organic solar cells. However, it was found that benzodithiophenes undergo photooxidative degradation at the 4- and 8-position.[9] As it is known for acenes, in particular pentacene, introduction of nitrogens into the conjugated π-system lower the HOMO energy level without influencing the planarity of the molecule.[10–14] Consequently, N-heteroacenes are more air-stable and possess higher electron transport efficiency.[10,15,16]

In this respect, Hayashi *et al.* could show by quantum chemical calculations that the introduction of nitrogen(s) in *syn*- and *anti*-benzodithiophene **1** and **2**, represented in dithienopyridines **3** and **4** and in *syn*- and *anti*-dithienopyrazine **5** and **6** leads to a continuous decrease of both, the HOMO and the LUMO energy level (Figure 1).[17] We use the denomination „*anti*" and „*syn*" in order to represent regiochemical relationships in the triacenes. „*Anti*" means that the sulfur atoms of the fused thiophene rings are „on opposite sides" of a reference line/plane in the molecule, in contrast to „*syn*" which means „on the same side".[18]

The synthetic realization of the basic benzodithiophenes **1** and **2** is long known since the 1950th and various methods have been developed over the years.[19-25] In the case of N-heterotriacenes **3**-**6** typically substituted derivatives were prepared by different synthetic strategies [26-28,29-31] and only preparation of the basic *syn*-derivative, dithieno[3,2-*b*:2',3'-*e*]pyridine **3**, was described by Outurquin *et al*.[32] whereby the other unsubstituted heterotriacenes **4**-**6** are not literature-known up to now.

A versatile synthetic route to functionalized derivatives of triacenes **3** and **6** was reported in 2016 by Oechsle and Paradies.[33] In a twofold domino reaction consisting of Pd-catalyzed C-S coupling and subsequent base-induced *5-endo-dig*-cyclization of ethynylated 3,5-dichloropyridines or corresponding 3,5-dichloropyrazines, series of (hetero)-arylated dithieno[3,2-*b*:2',3'-*e*]pyridines and *syn*-dithieno[3,2-*b*:2',3'-*e*]pyrazines were obtained.

In this communication, we now describe synthesis and structural characterization of unknown basic *anti*-dithieno[2,3-*b*:2',3'-*e*]pyrazine **5** and isomeric *syn*-dithieno[2,3-*b*:3',2'-*e*]pyrazine **6** as valuable building blocks for further transformations. Their reactivity in follow-up reactions such as electrophilic substitution, lithiation, or redox reactions was investigated which led to a manifold of novel derivatives.

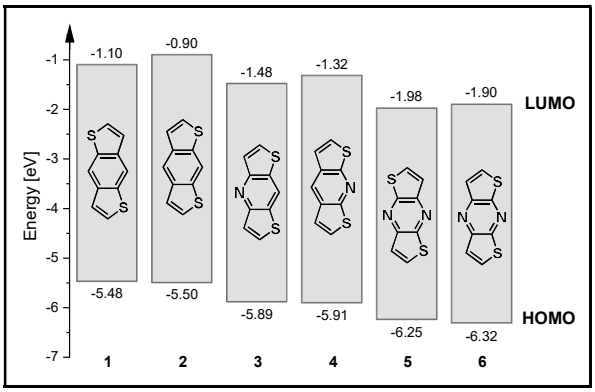

Figure 1: Calculated HOMO and LUMO energy levels of heterotriacenes **1**-**6**.[17]

Results and Discussion

Synthetic Procedures. For the synthesis of the targeted isomeric dithienopyrazines **5** and **6** we chose and further developed the C-S coupling and cyclization of ethynylated pyrazines with sulfurization reagents introduced by Oechsle and Paradies. Thus, in the first step 2,6-dibromo-3,5-dichloropyrazine **7**[33,34] was efficiently reacted in a Pd/Cu-catalyzed Sonogashira-type cross-coupling with tri*iso*propyl (TIPS)-protected acetylene **8** to targeted 2,6-dichloro-3,5-bis[(triisopropylsilyl)ethynyl]pyrazine **9** in 96% yield as precursor for the subsequent *5-endo-dig*-cyclization to the *syn*-dithieno[2,3-*b*:3',2'-*e*]pyrazine core according to the Baldwin rules.[35] Pyrazine **9** was cyclized Pd/ligand-free to TIPS-protected *syn*-dithieno[2,3-*b*:3',2'-*e*]pyrazine **10** with potassium thioacetate (KSAc) as sulfur source in acetone in 82% yield. Optimization of this reaction revealed that in total six equivalents of KSAc gave the best yield of the targeted pyrazine **10** and lowest amount of side products. The final step was the fluoride-induced deprotection and cleavage of the silyl groups with tetrabutylammonium fluoride to give parent *syn*-dithieno[2,3-*b*:3',2'-*e*]pyrazine **6** in nearly quantitative yield (Scheme 1).

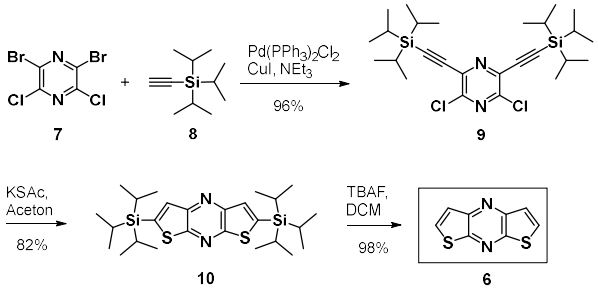

Scheme 1: Synthesis of *syn*-dithienopyrazine **6** starting from 2,6-dibromo-3,5-dichloropyrazine **7.**

Thus, by starting from commercially available 2-amino-6-chloropyrazine, the target compound was obtained in 73% overall yield in five steps. This procedure allowed to up-scale the reaction sequence and the products were prepared on the gram-scale. First attemps to use trimethylsilyl-protected analogues as precursors or other sulfur sources for the ring closure reaction resulted in various complications such as thioethers as main or side products.[36]

For the synthesis of isomeric *anti*-dithienopyrazine **5** the same strategy was chosen and 2,5-dibromo-3,6-dichlorpyrazine **11**, which is isomeric to halogenated pyrazine **7**, was synthesized starting from 2-amino-6-chloropyrazine according to literature and patent procedures.[37,38] Pd/Cu-catalyzed Sonogashira-type coupling of **11** with TIPS-acetylene **2** gave twofold ethynylated pyrazine **12** in 98% yield which was cyclized with KSAc in acetone (75% yield) and deprotected nearly quantitatively to targeted *anti*-dithienopyrazine **5** (Scheme 2). In this case, as well starting from the commercially available 2-amino-6-chloropyrazine a lower overall yield of 41% was obtained due to the more tedious preparation of tetrahalogenated pyrazine **11**.

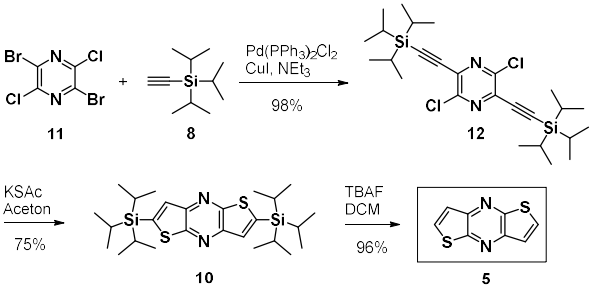

Scheme 2: Synthesis of *anti*-dithienopyrazine **5** starting from 2,5-dibromo-3,6-dichloropyrazine **11**.

The structures of the novel pyrazines and dithienopyrazines were fully characterized by NMR-spectroscopy and high-resolution mass spectra (HRMS). The ^{1}H-NMR spectra of the targeted isomeric dithienopyrazines **5** and **6** are nearly identical and show two doublets at 7.88(9) ppm und 7.54(3) ppm with a ^{3}J coupling constant of 6.2 Hz and correspond to the α- (H2) and β-protons (H3) of the fused thiophene units, respectively. This α,β-H-coupling constant is larger than for other thiophene-fused acenes, such as thieno[2,3-*b*]pyrazine (6 Hz),[39] thieno[2,3-*b*]pyridine (5.9 Hz),[40] or benzodithiophene (5.5 Hz).[41] The assignment of the protons and resulting $^{1}J_{CH}$ coupling constants were taken on the basis of non-decoupled heteronuclear single quantum coherence (HSQC) NMR spectra (*vide ultra*). The ^{13}C-NMR spectra of the targeted isomeric dithienopyrazines **5** and **6** are as well nearly identical and show four signals. Two of

them at 146-154 ppm are assigned to the quaternary carbons (C4 and C5), those at higher field at 132 ppm to the tertiary α-(C2) and at 122 ppm to the β-carbons (C3) of the fused thiophene units. The assignment of the tertiary carbons was taken on the basis of non-decoupled HSQC spectra.

Determination of the optoelectronic properties of the novel dithienopyrazines **5** and **6** revealed absorption maxima at 336 and 339 nm, respectively, and emissions at 379 nm in dichloromethane (DCM). Redox potentials, which were determined by cyclic voltammetry in DCM/tetrabutylammonium hexafluorophosphate (0.1 M), gave irreversible oxidation waves with peak potentials at E_p^{Ox} = 1.52 V and 1.63 V vs ferrocene/ferricenium (Fc/Fc^+) and reversible reduction waves with half wave potentails at $E_{1/2}^{Red}$ -2.19 V for both derivatives (Table 1). HOMO and LUMO energies were determined using these potentials and setting the reference redox couple Fc/Fc^+ at -5.1 eV vs vacuum level. Thus, for the *anti*-derivative **5** a E_{HOMO} level of -6.48 eV, a E_{LUMO} level of -3.02 eV, leading to an energy gap E_g of 3.46 eV were determined. In the same way, the values for *syn*-derivative **6** were only marginally different and resulted in E_{HOMO} = -6.56 eV, E_{LUMO} = 3.04 eV, and E_g = 3.52 eV. Compared to the calculated HOMO and LUMO energy levels of heterotriacenes **5** and **6**[17] (*vide supra*), our experimental data is in approximate agreement for the HOMO energies, but differ substantially for the LUMO energies, which are vastly overestimated by the calculations. Consequently, the energy gaps were also calculated oversized.

Dithienopyrazine	E_p^{Ox} [V]	$E_{1/2}^{Red}$ [V]	E_{HOMO} [eV]	E_{LUMO} [eV]	E_g [eV]
5 (exp.)	1.52	-2.19	-6.48	-3.02	3.46
5 (calc.)	-	-	-6.25	-1.98	4.27
6 (exp.)	1.63	-2.19	-6.56	-3.04	3.52
6 (calc.)	-	-	-6.32	-1.90	4.42

Table 1. Experimental redox potentials, HOMO/LUMO energies, and electrochemical energy gaps of dithienopyrazines **5** and **6** in comparison to calculated data.[17]

Nevertheless, these results showed that the formal introduction of nitrogens into the benzodithiophene core led to a stabilization of both, HOMO and LUMO, by around 0.7-0.8 eV each in the dithienopyrazines transforming them to rather electron-deficient and less oxidation sensitive systems. These electronic properties become important for their reactivity in follow-up reactions, which is described in the chapter below.

Reactivity and Follow-up Reactions

Halogenation reactions. The successful synthesis of the basic heterotriacene structures **5** and **6** allowed for the investigation of possible follow-up reactions in order to widen the scope of corresponding derivatives. Since there is a restricted number of publications describing reactivities of triacenes, we studied electrophilic substitution, metallation, and redox reactions on dithienopyrazines **5** and **6** and compared reactivities, regioselectivities, and product spectrum.

Halogenation is a viable way to receive activated derivatives, which subsequently can be used for further functionalization by, e.g., transition metal-catalyzed C-C cross-coupling reactions. In this respect, electrophilic bromination of *anti*-benzo[1,2-*b*:4,5-*b'*]dithiophene **1** with N-bromosuccinimide (NBS) led to bromination of the α-positions of the fused thiophenes in only 34% yield.[42] The yield increased to 60% for the NBS-bromination of 4,8-dihexylbenzo[1,2-*b*:4,5-*b'*]dithiophene.[43] If elemental bromine as stronger electrophile is used, 4,8-dioctyloxybenzo[1,2-*b*:4,5-*b'*]dithiophene is brominated in the 2,6-positions in 99% yield.[44] NBS-bromination of isomeric *syn*-benzo[1,2-*b*:5,4-*b'*]dithiophene **2** led to an inseparable mixture of differently brominated products.[25]

Structurally related to our dithienopyrazines, thieno[2,3-*b*]pyridine, thieno[3,2-*b*]pyridine, or thieno[2,3-*b*]pyrazine are throughout halogenated with elemental bromine or chlorine at the fused thiophene β-position in moderate to good yields. The only information about bromination of dithienopyrazines is specified in a Chinese patent. Therein, it is claimed that NBS-bromination of *anti*-dithienopyrazine **5** should result in α,α'-dibrominated 2,6-dibromodithieno[2,3-*b*:2′,3′-*e*]pyrazine in 93% yield.[45]

In our hands, NBS was too weak as a bromination agent for dithienopyrazines **5** and **6**. Under various reaction conditions, even harsh ones, practically no product formation was observed. Only the use of elemental bromine in the presence of Brönsted (HBr) or Lewis acidic conditions ($AlCl_3$), which are the typical reaction conditions for electrophilic substitutions of moderately activated aromatics such as benzene, led to controlled twofold and tetrafold bromination (Scheme 3). For the synthesis of dibrominated pyrazine **14** six equivalents of bromine in a solution of HBr in acetic acid and chloroform were used and the reaction mixture was heated under reflux for 7 days leading to 91% yield. After tedious optimization of solvents and temperature

for the synthesis of tetrabrominated pyrazine **15** a great excess of bromine and aluminum trichloride ($AlCl_3$) was used and the reaction conducted at 75 °C for one day finally leading to 92% yield. The various reaction conditions showed that the dithienopyrazine system is rather electron-deficient leading to a moderate reactivity in electrophilic substitution reactions.

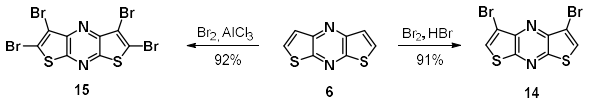

Scheme 3: Bromination of *syn*-dithienopyrazine **6**.

For comparison to the *syn*-isomer **6**, the reactivity of *anti*-dithienopyrazine **5** in electrophilic substitution reactions was investigated and the optimized reactions transferred. The highly effective bromination protocol gave corresponding dibrominated and tetrabrominated products **16** and **17** in 88% and 76% yield, respectively (Scheme 4). Also in this case, NBS-bromination was not effective and only led to marginal formation of bromination products. Therefore, the claimed results of the patent could not be reproduced (*vide supra*).[45]

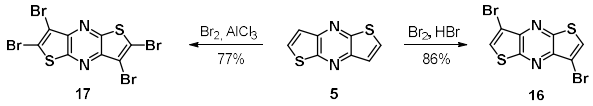

Scheme 4: Bromination of *anti*-dithienopyrazine **5**.

Metallation reactions. The regioselectivity of metallations at triacene cores might be different compared to that of electrophilic substitutions. Structurally related to the dithienopyrazines, thieno[2,3-*b*]pyridine,[46,47] thieno[3,2-*b*]pyridine,[48] and triacenes benzodithiophene[49] and dithieno[3,2-*b*:2',3'-*e*]pyridine[50] are typically lithiated at the α-position(s). Therefore, we were interested in the metallation selectivity of our dithienopyrazines **5** and **6** and investigated their lithiation and subsequent intercepting reactions such as halogenation and transmetallation (Scheme 5).

Firstly, in a test reaction, we used a series of bases with decreasing strength as lithiation reagent: *tert*-BuLi (pK_a = 53), *sec*-BuLi (pK_a = 51), *n*-BuLi (pK_a = 50), MeLi (pK_a = 48) and PhLi (pK_a = 43).[51,52] The weakest base phenyl lithium (PhLi) gave the best results with respect to the yield of dilithiated product, which was quenched with trimethylsilylchloride (50%), and to the lowest portion of decomposition of the substrate (4%). In contrast, with the strongest base *tert*-BuLi no product was obtained and 100% of the starting material were decomposed. The other bases gave intermediate results. Further optimization of the lithiation reaction of dithienopyrazine **6** with PhLi as base in THF at -95°C and tetrabromomethane as quenching reagent gave 2,6-dibromo derivative **18** in 83% yield. Similarly, lithiation of **6** with PhLi in THF at -78°C and quenching with elemental iodine was likewise effective and corresponding 2,6-diododerivative **19** was obtained as well in 83% yield. In both cases, small amounts of mono-substituted product were easily removed by column chromatography. Besides the lithiation/halogenation sequence, transmetallation of the intermediate diltihiated dithienopyrazine **6** was undertaken with tributylstannylchloride and bis-stannylated *syn*-dithienopyrazine **20** was isolated in 79% yield. Analogous lithiation of isomeric dithienopyrazine **5** with PhLi as base in THF at -95°C and tetrabromomethane as quenching reagent gave the 2,6-dibromo derivative **21**. Due to the lower solubilty of the *anti*-derivative **5** in THF compared to **6** a substantially higher dilution was necessary. This obviously led to a lower yield of 38% of dibrominated **21** whereby in this case a monobrominated derivative was isolated as a side product in 26% yield.

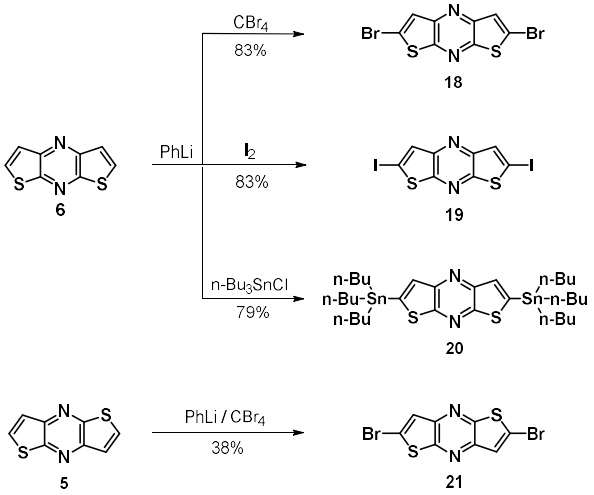

Scheme 5: Llithiation and follow-up reactions of *syn*-dithienopyrazine **6** and *anti*-dithienopyrazine **5**.

These investigations showed that by electrophilic halogenation and the lithiation/halogenation sequence different substitution patterns at the dithienopyrazines **5** and **6** were achieved: direct halogenation leads to β,β-substitution, the latter procedure to α,α-substituted derivatives. Structural proofs were made by NMR and single crystal X-ray structure analysis and are discussed below.

Redox reactions, reductions. It was the question if the dithienopyrazine system as aromatic system can be reduced or oxidized. Precedents in literature are scarce and for example related phenazine was reduced to corresponding 5,10-dihydrophenazine with sodium dithionite. The reduction obviously occurs at the central pyrazine ring, whereby the dihydrophenazine exhibits strong oxidation sensitivity.[53] Furthermore, the reactive nitrogens in the pyrazine ring can be N-alkylated after *in-situ* reduction[54] or acylated.[11]

Reductions of thiophene-fused pyrazines are not literature-known. Therefore, we wanted to investigate reduction possibilities of *syn*-dithienopyrazine **6**. In this respect, reducing agents such as sodium dithionite or elemental sodium/alkylation agent did not lead to the corresponding dihydropyrazines and starting material was reisolated. Next, TIPS-protected *syn*-dithienopyrazine **10** and *syn*-dithienopyrazine **6** were subjected to reductive acylation conditions and heated under reflux with elemental zinc in acetic anhydride. N-diacylated *syn*-dihydrothienopyrazines **22** and **23** were isolated in quantitative and 93% yield, respectively. Acylated dihydrothienopyrazine **23** was furthermore brominated with NBS at room temperature under the exclusion of light leading to 2,6-dibromoderivative **24** in 53% yield (Scheme 6).

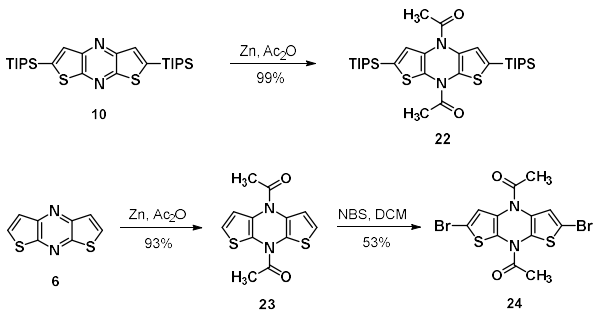

Scheme 6: Reductive acylation of *syn*-dithienopyrazines **4** and **5**.

The obtained substitution pattern was proven by NMR methods and showed that in contrast to the fused aromatic *syn*-dithienopyrazine **6**, which was regioselectivly brominated at the β-positions, dibromination of dihydrothienopyrazine **23** is α-selective. Therefore, it can be regarded as nitrogen-bridged aromatic thiophenes, which are typically substituted with electrophiles at the α-position.[55] This result is also rationalized by the fact that for the bromination of dihydrothienopyrazine **23** much smoother reaction conditions were necessary compared to those of dithienopyrazine **6**.

Oxidation reactions. Since reductions of our dithienopyrazines worked well and selective, we investigated their oxidation behaviour. Regarding the subunits of the triacene system, thiophenes typically can be oxidized to rather labile thiophene 1-oxides and further to stable thiophene 1,1- or S,S-dioxides,[56] whereby nitrogen-containing heterocycles such as pyridine or pyrazine are oxidized to N-oxides.[57] Thus, oxidation of structurally related 2-phenyl thieno[2,3-*b*]pyrazine with 30% hydrogen peroxide (H_2O_2) solution in acetic acid showed that depending on temperature a N-oxide, N,N-dioxide, and a combined thiophene 1,1-dioxide N-oxide are formed.[58] On the other hand, it has been shown that depending on the oxidant thienopyridines can be selectively oxidized at the nitrogen or at the sulfur. Thus, oxidation with H_2O_2 in acetic acid or m-chloroperbenzoic acid in chloroform led to the corresponding pyridine N-oxid,[59,60] oxidation with sodium hypochlorite in diluted hydrochloric acid to the 1,1-dioxide.[61] Structural proofs came from ^{1}H-NMR and IR data. In this respect, thiophene 1,1-dioxide units show much larger coupling constants (7-7.5 Hz) for the thiophene α,β-protons[62] than thiophene units itself (5.6-5.9 Hz).[40,63] Furthermore, in IR spectra of sulfones a characteristic symmetric stretching band arise in the regime of 1135-1170 cm^{-1}, an asymmetric one between 1300-1335 cm^{-1}.[64] In contrast, for aromatic N-oxides a stretching band in the regime of 1200-1300 cm^{-1} is expected.[65]

In analogy, we tested oxidation of *syn*-dithienopyrazine **6** with 30% H_2O_2 in acetic acid at 60 °C and a mixture of pyrazine-4-N-oxide **25**, 1,1-dioxide **26**, and pyrazine-4-oxide-1,1-dioxide **27** was identified. After chromatographic separation, the three oxidation products were isolated in rather moderate yields from 10% to 23%. Replacement of acetic acid by the stronger trifluoroacetic acid as solvent and reaction at 100 °C gave after work-up as well pyrazine-4-oxide-1,1-dioxide **27** and the higher oxidized pyrazine-4,8-dioxide-1,1-dioxide **28** in quite moderate yields (Scheme 7). The structures and assignments of the various oxidation products comprising positions of the oxygens were discerned and determined by high resolution mass (HR-MS), ^{1}H-NMR and IR spectra, and as well single crystal X-ray structure analysis. In that respect, thiophene-1,1-dioxide units are clearly identified by the ^3J coupling constants of the α,β-thiophene protons which are increased to 7.8-7.9 Hz compared to 6.2 Hz of the non-oxidized thiophene units. Furthermore, absorption bands at

1155-1163 cm^{-1} and 1311-1325 cm^{-1} in the IR-spectrum can be assigned to a sulfone (1,1-dioxide) unit. In contrast, oxidation of nitrogens to N-oxides in the triacene systems can be discerned in the IR-spectrum by absorption bands at lower energies (1241-1260 cm^{-1}). The undertaken experiments showed that *syn*-dithienopyrazine **6** can only be oxidized under tightened conditions and non-selective mixtures of mono to fourfold oxidized products were formed.

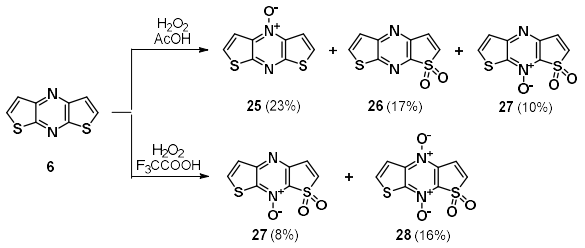

Scheme 7: Oxidation reactions of *syn*-dithienopyrazine **6.**

*Transition metal-catalyzed cross-coupling reactions of brominated syn-dithienopyrazines **14**, **15**, and **18**.* The application of the novel dithienopyrazines as building blocks in electronic organic materials requries efficient cross-coupling reactions in order to build up tailored π-conjugated systems. In that respect, we elaborated the Pd-catalyzed Suzuki-type coupling of brominated *syn*-dithienopyrazines **14**, **15**, and **18** with TMS-substituted thiophene boronic ester **29** in order to elongate the dithienopyrazine system with additional thiophene units at different positions of the triacenes (Scheme 8). As catalytic system tris(dibenzylideneaceton)dipalladium (Pd_2dba_3) and tri-*tert*-butylphosphonium tetrafluoroborate [$HP(t\text{-}Bu_3)BF_4$] as ligand, and potassium carbonate as base was used in a mixture of THF and water. Dibromides **14** and **16** did not show differences in reactivity under the same reaction conditions (15 hr at r.t.). 3,5-Dithienylated dithienopyrazine **30** was isolated in 73% and the 2,6-disubstituted isomer **31** in 70% yield. The fourfold coupling reaction of tetrabrominated derivative **15** required somewhat more drastic conditions (22 hr at 60 °C) and delivered tetrathienylated **31** in 60% yield.

Similar efficient worked the extension of the basic structure with ethynyl groups and TMS-protected acetylene **33** was subjected to Sonogashira-Hagihara-type coupling reactions with the same brominated *syn*-dithienopyrazines **14**, **15**, and **18**. Bis(triphenylphosphine)palladium(II) chloride ($(PPh_3)_2Cl_2$) and copper iodide were used as catalytic system and triethylamine and toluene served as solvent. For this type of cross-coupling reaction we noted differences in reactivity, whereby the α,α'-dibrominated dithienopyrazine **18** was substantially more reactive than the β,β'-dibrominated derivative **14**. 2,6-Diethynylated derivative **34** was isolated in 96% and the reaction was completed after 18 hours at room temperature, the 3,5-diethynylated isomer **35** was isolated in 68% yield after reaction at 50 °C and 48 hours reaction time. Tetrabrominated dithienopyrazine **15** needed harsher reaction conditions (24 hrs at 110 °C) to provide tetraethynylated derivative **36** in 70% yield (Scheme 9).

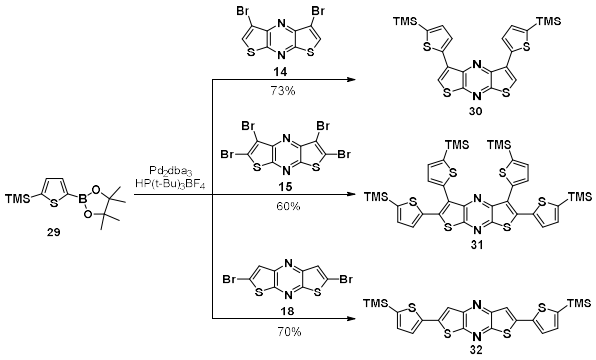

Scheme 8: Suzuki-type cross-coupling reactions of brominated *syn*-dithienopyrazines **14**, **15**, and **18**.

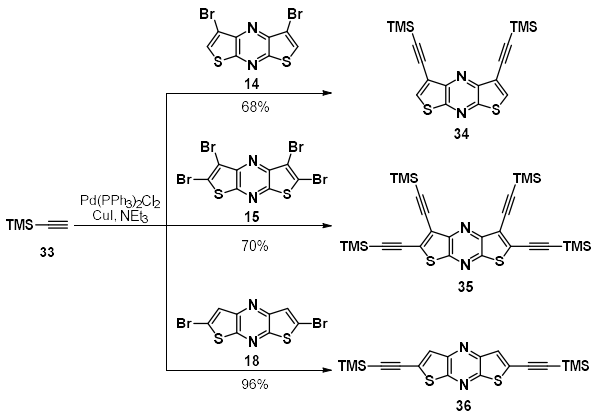

Schema 9: Sonogashira-type cross-coupling reactions of brominated *syn*-dithienopyrazines **14**, **15**, and **18**.

These transition metal-catalyzed Suzuki and Sonogashira-type coupling reactions, which were optimized for the brominated *syn*-dithienothiophenes **14**, **15**, and **18**, were as well applied to the corresponding *anti*-derivatives **16**, **17**, and **21** in order to prepare series of triarylamino-functionalized dithienothiophenes as potential hole-transport materials for perovskite solar cells. The results will be reported in a forthcoming paper.

Structural characterization by NMR, determination of regioselectivity. For the assignment of the substitution positions and residual protons, non-decoupled heteronuclear single quantum coherence (HSQC) NMR spectra were taken and the resulting $^1J_{CH}$ coupling constants determined. Klemm *et al.* showed that in a fused thiophene ring the $^1J_{CH}$ coupling constant for the α-position (C_2-H_2, signal at lower field) always is larger than this for the β-position (C_3-H_3, signal at higher field) due to the vicinity to the sulfur.[62] Therefore, for comparison HSQC NMR spectra of the basic dithienopyrazines **5** and **6** were recorded and $^1J_{CH}$ coupling constants of 194/190 Hz were determined for the α-proton signals at δ = 7.89 ppm and 176/177 Hz for the β-proton signals at δ = 7.57/7.53 ppm. Therefore, we were able to unequivocally distinguish the substitution pattern in various follow-up products which are collected in Table 2.

As a general result, we found that reactivity and regioselectivity of the two isomeric dithienopyrazines **5** and **6** selectively occur at the β-positions for electrophilic bromination reactions, whereby metallations are directed to the α-positions.

Table 2. $^1J_{CH}$ coupling constants and regioselectivities of various dithienopyrazines.

Dithieno-pyrazine	*syn/anti*	$^1J_{CH}$ [Hz]	δ [ppm]	Proton assignm.	Substit. position
5	*syn*	194	7.89	α	-
		176	7.57	β	-
6	*anti*	190	7.89	α	-
		177	7.53	β	-
14	*syn*	196	7.99	α	β
18	*syn*	179	7.59	β	α
16	*anti*	192	7.94	α	β
21	*anti*	179	7.52	β	α

Structural characterization by single crystal X-ray structure analysis. Single crystals were obtained for three different structures by recrystallization and analyzed by X-ray structure analysis: *syn*-dithienopyrazine **10**, *anti*-dithienopyrazine **5**, and *syn*-dithienopyrazine-4-oxide **25**. In Figure 2, individual molecules with atom numbering scheme are shown from top and side view.

Whereas *syn*-dithienopyrazines **10** and **25** crystallized in orthorhombic space groups ($P2_12_12$ and Pbca, resp.) with 4 and 8 molecules in the unit cell, *anti*-configured dithienopyrazine **5** crystallized in the monoclinic space group $P2_1/n$ with 2 molecules in the unit cell. The heterocyclic triacene π-systems are as expected fully planar. We shortly discuss the most obvious general trends for bond lengths and angles compared to the basic heterocycles thiophene,[55] pyrazine,[66,67] and pyrazine-N-oxide.[68] More details can be found under the corresponding CCDC-numbers.

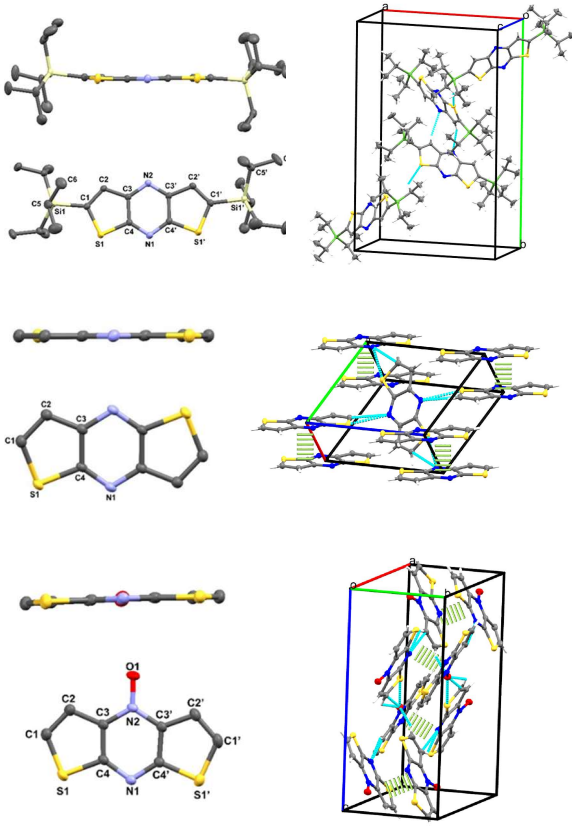

Figure 2: Single crystal X-ray structure analysis of TIPS-protected *syn*-dithienopyrazine **10** (CCDC-number 2001337) (top), *anti*-dithienopyrazine **5** (CCDC-number 2001367) (middle), and *syn*-dithienopyrazine-4-oxide **25** (CCDC-number 2001336) (bottom). Single molecules with atom numbering scheme in top view (bottom, each) and side view (top, each). Unit cell with labelled intermolecular interactions below the sum of the van der Waals radii (right, each): N-X, O-X, and S-X short interactions between herringbone-oriented molecules (cyan dashed lines) and π–π intermolecular interactions (green bars).

We note that due to the fusion of the heterocycles, the central part significantly stretches perpendicular to the long axis compared with the basic heterocycles: on one side thiophene S1-C1 and S1-C4 bonds (correspondingly S1'-C1' and S1'-C4') are elongated (1.74-1.76 Å) compared to thiophene (1.71 Å). The pyrazine N1-C4 (N1'-C4') bonds are as well elongated (1.34-1.36 Å) compared to pyrazine (1.31 Å). On the other side, the C3-C4 (and C3'-C4') bond lengths (1.41-1.43 Å), which belong to both heterocycles in the triacenes and represent the fusing bonds, were substantially longer than in the underlying thiophene or pyrazine (1.37 Å), therefore indicating less double bond character. Concomitantly, the C4-N1-C4' angles in

the central pyrazine unit of the *syn*-derivatives **10** and **25** are compressed to 112° compared to pyrazine with 115°. The angle reduction is, nevertheless, less pronounced for *anti*-derivative **5** (114°) and for the opposite C3-N2-C3' angle (114°) in **10**. In contrast, this angle is widened to 117° in N-oxide **25** due to the increased sp^2-character of the oxidized unit $N2^+$-$O1^-$ which is rather typical for pyrazine-N-oxide (118°).[68] All other bond lengths and angles are not significantly different compared to the parent heterocycles.

Concerning the packing motifs in the crystal, a herringbone-like arrangement of the molecules (herringbone angle of 83°, 110°, and 123° for **10**, **5**, and **25**, respectively) gives rise to intermolecular interactions with short heteroatomic S-C, S-N, S-O, C-N, and C-S distances, far below the sum of corresponding van der Waals radii (Figure 2 right, each, cyan dashed lines). In addition, strong $\pi-\pi$ interactions between molecules at distances as short as 3.32 Å and 3.28 Å have been found for *anti*-derivative **5** and N-oxide **25**, respectively (green bars).

Conclusion

We showed a straightforward and efficient method for the preparation of the so far unknown parent *anti*- and *syn*-dithienopyrazines **5** and **6** including a Pd and ligand-free C-S coupling reaction of ethynylated precursors. The investigation of their electronic properties clearly show stabilization of HOMO and LUMO energy levels and little differences for the two isomers compared to benzodithiophenes and dithienopyridines. This circumstance has consequences on reactivity and regioselectivity of the rather electron-deficient triacenes in, *e.g.*, halogenation, metallation, and redox reactions which allowed for the preparation of valuable halogenated precursors of various substitution patterns for subsequent C-C cross-coupling reactions. To this end, *anti*- and *syn*-dithienopyrazines may become reasonable and versatile (acceptor) synthons with potential for novel organic electronic materials. In an upcoming communication we demonstrate that this concept leads to efficient hole-transport materials for perovskite solar cells.

Experimental Section

Instruments and methods. NMR spectra were recorded on an Avance 400 (^{1}H NMR 400 MHz, ^{13}C NMR 101 MHz) or a Bruker AMX 500 spectrometer (^{1}H NMR 500 MHz, ^{13}C NMR 125 MHz) at 293 K. Chemical shifts (δ) are reported in ppm using residual solvent protons (^{1}H NMR: δ_H = 7.26 for $CDCl_3$; ^{13}C NMR: δ_C = 77.2 for $CDCl_3$) as internal standard. The splitting patterns are designated as follows: s (singlet), d (doublet), dd (doublet of doublet), t (triplet), and m (multiplet). Coupling constants *J* relate to proton-proton couplings and assignments were made according to the nomenclature numbering scheme. High resolution MALDI mass spectra were performed on a Bruker SolariX using trans-2-[3-(4-*tert*-butylphenyl)-2-methyl-2-propenylidene]malononitrile (DCTB) as matrix. High resolution ESI spectra were performed on a Bruker SolariX using acetonitrile as solvent. The calculated and measured m/z values relate to the monoisotopic masses. GC-MS measurements were performed on a Shimadzu GCMS-QP2010 SE equipped with an Optima 5MS column (30 m x 0.25 mm) from Macherey-Nagel. The samples were ionized by electron impact (EI). GC measurements were performed on a Shimadzu GC-2010 Plus gas chromatograph with hydrogen as carrier gas.

Thin layer chromatography was carried out on aluminum plates, precoated with silica gel, Merck Si60 F254. Preparative column chromatography was performed on glass columns packed with silica gel (particle size 40-63 μm) from Macherey-Nagel or aluminum oxide, Merck 90 active basic, particle size 63-200 μm. HPLC were conducted on a Shimadzu CBM-20A equipped with a SPD-20A UV-vis detector, a LC-8A-solvent facility, and a column Nucleosil 100-5 NO_2 from Macherey-Nagel.

Melting points were determined on a Büchi B-565 apparatus. IR spectra were taken on a compact FTIR spectrometer ALPHA II with an Eco-Platinum ATR module.

Optical measurements in solution were carried out in 1 cm cuvettes with Merck Uvasol grade solvents. Absorption spectra were recorded on a Perkin Elmer Lambda 19 Spectrometer UV-vis-nir spectrophotometer. Fluorescence spectra were recorded on a Perkin Elmer LS 55 Luminescence Spectrometer.

Cyclic voltammetry experiments were performed with a computer-controlled Autolab PGSTAT30 potentiostat in a three-electrode single-compartment cell (5 mL). The platinum working electrode consisted of a platinum wire sealed in a soft glass tube with a surface of A = 0.785 mm^2, which was polished down to 0.25 μm with Buehler polishing paste prior to use to guarantee reproducible surfaces. The counter electrode consisted of a platinum wire and the reference electrode was an Ag/AgCl

reference electrode. All potentials were internally referenced to the ferrocene/ferricenium couple (Fc/Fc^+). For the measurements, concentrations of 10^{-3} M of the electroactive species were used in freshly distilled and deaerated dichloromethane (Lichrosolv, Merck) purified with a solvent purification equipment MB-SPS-800 from MBraun. Tetrabutylammonium hexafluorophosphate (Sigma-Aldrich, recrystallized twice from ethanol) was applied as the supporting electrolyte in a concentration of 0.1 M and the solution was blanketed with argon during the measurements.

X-ray diffraction data of single crystals were collected on a Bruker D8 Quest single crystal diffractometer equipped with a PHOTON II-Detektor and Mo-K_α-irradiation (wavelength λ = 0.71073 Å). Data collection, data reduction, and cell refinement were performed using the CrysAlisPro software.[69] An absorption correction based on the semi-empirical "multi-scan" approach was performed using the SCALE3 ABSPACK scaling algorithm.[69] The structure was solved by charge flipping using Superflip.[70-72] For the final model all non-hydrogen atoms were refined anisotropically using SHELXL.[73]

Materials. Acetic acid, acetone, acetonitrile (ACN), chloroform, dichloromethane (DCM), diethyl ether, dimethylsulfoxide, ethyl acetate (EA), ethanol, *n*-hexane, *iso*-propanol, methanol, petroleum ether (PE), and tetrachloroethane were purchased from Avantor. Toluene and tetrahydrofuran (THF) were purchased from Sigma Aldrich. Typically, the solvents were dried and purified by a MB SPS-800 solvent purification equipment from MBraun. The following chemicals were used: aluminum trichloride (Merck), 2-amino-6-chloropyrazine (Fluorochem), ammonium chloride (Avantor), elemental bromine (Sigma Aldrich), acetic acid anhydride (Avantor), HBr 33% solution in acetic acid (Merck), H_2O_2 33% solution in water (Avantor), iodine (Merck), isoamylnitrite (Alfa Aesar), potassium carbonate (Avantor), potassium thioacetate (Alfa Aesar), copper iodide (Merck), magnesium sulfate (Alfa Aesar), sodiumhydrogensulfite (Avantor), sodium hydroxide (Avantor), sodium nitrite (Merck), *N*-bromosuccinimid (Merck), *N*-chlorosuccinimide (Merck), phenyl lithium 1,9 M solution in dibutyl ether (Sigma Aldrich), tetrabromomethane (Alfa Aesar), tributyltin chloride (Merck), trifluoroacetic acid (Merck), $Pd(dba)_2$ (Sigma Aldrich), $HP(tBu)_3BF_4$ (Sigma Aldrich), $Pd_2(dba)_3$ (Sigma Aldrich), $Pd(PPh_3)_2Cl_2$ (TCI), zinc powder (Acros Organics), tri*iso*propylsilylacetylene **8** (Apollo), trimethylsilylacetylene **33** (Karl Bucher GmbH), tetrabutylammonium fluoride (Fluorochem). Triethylamine (Merck) was dried over phosphorous pentoxide (Sigma Aldrich) and distilled. 2,6-Dibromo-3,5-dichloropyrazine **7**,[33] 2,5-dibromo-3,6-dichloropyrazine **11**,[37] and tetramethyl[(1,3,2-dioxaborolan-2-yl)thien-2-yl]silane **29**[74] were prepared according to literapture procedures.

Synthetic Methods.

*2,6-Dichloro-3,5-bis[(triisopropylsilyl]ethynyl)pyrazine **9***. 2,6-Dibromo-3,5-dichloropyrazine **7** (20.0 g, 65.2 mmol), $Pd(PPh_3)_2Cl_2$ (2.3 g, 3.3 mmol, 5.3 mol%), CuI (62 mg, 0.3 mmol, 0.5 mol%) were dissolved in toluene (abs) (240 mL) and degassed with argon for 30 min. Subsequently, triethylamine (55 mL) was added and the reaction mixture was degassed for further 10 min. Then, tri*iso*propylsilylacetylene **8** (30.0 mL, 134 mmol) was added at once and the reaction mixture heated for 4 hr at 80 °C. The solvents were removed and the residue purified by column chromatography (flash silica gel, PE/DCM 8:1). Pyrazine **3** was obtained as a greyish solid (32.0 g, 62.8 mmol, 96%). Mp 54.0-54.8 °C. ^{1}H-NMR (400 MHz, CD_2Cl_2): δ 1.31-0.98 ppm (m, 42H, Si(C*H*-(CH_3)$_2$)$_3$); ^{13}C-NMR (100 MHz, CD_2Cl_2): δ 147.5, 136.8, 104.0, 100.1, 18.9, 11.7 ppm. HRMS (ESI): m/z: calcd for $C_{26}H_{42}Cl_2N_2Si_2$+H^+ 509.2336 $[M+H]^+$; found: 509.2330 (δm/m = 1.24 ppm).

*2,6-Bis(triisopropylsilyl)dithieno[2,3-b:3',2'-e]pyrazine **10**.* To a solution of 2,6-dichloro-3,5-bis[(tri*iso*propylsilyl]ethynyl)pyrazine **9** (0.5 g, 1.0 mol) in acetone (40 mL) potassium thioacetate (0.45 g, 3.95 mmol) was added at once and the reaction mixture stirred for 5 hr at r.t. and additionally for 64 hrs at 50 °C. After 16 hr and 40 hr additional potassium thioacetate (225 mg, 1.97 mmol) was added. The solvent was removed and the residue purified by column chromatography (flash silica gel, PE/DCM 4:1). Pyrazine **10** (405 mg, 0.80 mmol, 82%) was isolated as a colorless solid. As a side product, a corresponding thioether, bis{6-[tri*iso*propylsilyl]-2-[(tri*iso*propylsilyl)ethynyl]thieno[2,3-*b*]pyrazin-3-yl}sulfan, was isolated (19.0 mg, 0.02 mmol, 4%). Mp 183.8-185.8 °C. ^{1}H-NMR (400 MHz, CD_2Cl_2): δ 7.72 (s, 2H, *H*-3), 1.47 (sep, $^3J_{HH}$ = 7.3 Hz, 6H, Si(C*H*-(CH_3)$_2$)$_3$)), 1.18 ppm (d, $^3J_{HH}$ = 7.3 Hz, 36H, CH_3); ^{13}C-NMR (100 MHz, CD_2Cl_2): δ 155.6, 148.8, 144.2, 131.5, 18.8, 12.2 ppm. HRMS (ESI): m/z calcd for

$C_{26}H_{44}N_2S_2Si_2+H^+$: 505.2557 $[M+H]^+$; found: 505.2558 (δm/m = 0,18 ppm).

Dithieno[2,3-b:3',2'-e]pyrazine ***6***. 2,6-Bis(tri*iso*propylsilyl)dithieno[2,3-*b*:3',2'-*e*]pyrazine **10** (2.3 g, 4.6 mmol) and tetrabutylammonium fluoride (3.6 g, 11 mmol) were dissolved in DCM (150 mL) and stirred for 3 hr at r.t. DCM was removed with the rotary evaporator and tri*iso*propylsilanol was distilled in vacuo. The obtained residue was purified by column chromatography (silica gel, DCM) and the product, dithienopyrazine **6** (0.86 g, 4.47 mmol, 98%), was obtained as a colorless solid. Mp 178.8-179.6 °C. ^{1}H-NMR (400 MHz, $CDCl_3$): δ 7.90 (d, $^3J_{HH}$ = 6.2 Hz, 2H, *H*-2), 7.56 ppm (d, $^3J_{HH}$ = 6.2 Hz, 2H, *H*-3); ^{13}C-NMR (100 MHz, $CDCl_3$): δ = 152.3, 147.5, 131.8, 122.6 ppm. HRMS (ESI): m/z calcd for $C_8H_5N_2S_2+H^+$: 192.9889 $[M+H]^+$; found: 192.9890 (δm/

2,5-Dichloro-3,6-bis[(triisopropylsilyl)ethinyl]pyrazine ***12***. 2,5-Dibromo-3,6-dichloropyrazine **11** (9.2 g, 30 mmol), CuI (28 mg, 0.2 mmol, 0.6 mol%) and $Pd(PPh_3)_2Cl_2$ (1.0 g, 1.5 mmol, 5.0 mol%) were suspended in toluene (150 mL) and degassed with argon for 30 min. Subsequently, triethylamine (25 mL) and tri*iso*propylsilylacetylene **8** (13.8 mL, 61.5 mmol) were added and the reaction mixture was heated at 80 °C for 2 hr. The solvent was removed in vacuo and the crude product purified by column chromatography (flash silica gel, PE/DCM 8:1). Pyrazine **12** (15.0 g, 29.4 mmol, 98%) was obtained as a colorless solid. Mp 121.5-124.1 °C. ^{1}H-NMR (400 MHz, $CDCl_3$): δ 1.24-1.17 (m, 6 H, Si-(C*H*)$_3$), 1.16-1.12 ppm (m, 36 H, C*H*$_3$). ^{13}C-NMR (100 MHz, $CDCl_3$): δ 147.9, 135.6, 105.9, 100.1 ppm. HRMS (ESI): m/z calcd for $C_{26}H_{42}Cl_2N_2Si_2+H^+$: 509.2336 $[M+H]^+$; found: 509.2334 (δm/m = 0.51 ppm).

2,6-Bis(triisopropylsilyl)dithieno[2,3-b:2',3'-e]pyrazine ***13***. To a solution of 2,5-dichloro-3,6-bis[(tri-*iso*propylsilyl)ethinyl]pyrazine **12** (7.0 g, 13.7 mmol) in acetone (250 mL) potassium thioacetate (23.5 g, 206 mmol) was added at 0 °C and the reaction mixture stirred for 1 hr in an ice bath. Subsequently, the reaction mixture was heated for 11 d at 50 °C. After cooling to r.t. the mixture was contracted to dryness and purified by column chromatography (flash silica gel, PE/DCM 4:1). Dithienopyrazine **13** (5.20 g, 10.3 mmol, 75%) obtained as a colorless solid. Mp 111.4-112.5 °C. ^{1}H-NMR (400 MHz, $CDCl_3$): δ 7.70 (s, 2H, *H*-3), 1.49-1.42 (m, 6H, Si(C*H*-(CH_3)$_2$)$_3$)), 1.17 ppm (d, $^3J_{HH}$ = 7.5 Hz, 36 H, C*H*$_3$); ^{13}C-NMR (100 MHz, $CDCl_3$): δ 156.4, 146.8, 145.1, 130.2 ppm. HRMS (ESI): m/z calcd for $C_{26}H_{44}N_2S_2Si_2+H^+$: 505.2557 $[M+H]^+$; found: 505.2551 (δm/m = 1.13 ppm).

Dithieno[2,3-b:2',3'-e]pyrazine ***5***. TIPS-protected dithienopyrazine **13** (2.3 g, 4.6 mmol) was dissolved in DCM (250 mL) and tetrabutylammonium fluoride (3.6 g, 11 mmol) was added and the mixture stirred for 16 hr at r.t. DCM was removed with the rotary evaporator and tri*iso*propylsilanol was distilled in vacuo. The residue was purified by column chromatography (flash silica gel, DCM) and dithienopyrazine **5** (0.94 g, 4.77 mmol, 96%) was obtained as a colorless solid. Mp 184.3-185.4 °C. ^{1}H-NMR (400 MHz, $CDCl_3$): δ 7.89 (d, $^3J_{HH}$ = 6.1 Hz, 2H, *H*-3), 7.53 ppm (d, $^3J_{HH}$ = 6.1 Hz, 2H, *H*-2); ^{13}C-NMR (100 MHz, $CDCl_3$): δ 154.0, 146.7, 132.6, 122.4 ppm. HRMS (ESI): m/z calcd for $C_8H_6N_2S_2+H^+$: 192.9889 $[M+H]^+$; found: 192.9891 (δm/m = 1.24 ppm).

3,5-Dibromodithieno[2,3-b:3',2'-e]pyrazine ***14***. Dithienopyrazine **6** (200 mg, 1.04 mmol) was dissolved in chloroform (20 mL) and hydrobromic acid (32-% in acetic acid, 10 mL) and elemental bromine (0.32 mL, 6.24 mmol) were added. The reaction mixture was heated for 7 d at 80 °C. After cooling, saturated sodium hydrogensulfite solution was added and the obtained residue was filtered. Chloroform was evaporated from the mother liquor and the precipitated solid was filtered. The combined and dried solid was purified by column chromatography (flash silica gel, PE/ DCM 1:1) and dithienopyrazine **14** (305 mg, 0.87 mmol, 84%) was obtained as a colorless solid. Mp 294.7-295.3 °C. ^{1}H-NMR (400 MHz, $CDCl_3$): δ 7.99 ppm (s, 2H, *H*-2); ^{13}C-NMR (125 MHz, $CDCl_3$) δ 151.5, 144.8, 129.2, 108.1 ppm. HRMS (ESI): m/z calcd for $C_8H_2Br_2N_2S_2+H^+$: 348.8099 $[M+H]^+$; found: 348.8093 (δm/m = 1.66 ppm).

2,3,5,6-Tetrabromodithieno[2,3-b:3',2'-e]pyrazine ***15***. Elemental bromine (10.0 mL, 195 mmol) was added to the furnished solids dithienopyrazine **6** (300 mg, 1.56 mmol) and aluminum trichloride (1.0 g, 7.8 mmol) and heated for 5 hr at 75 °C. After cooling, excessive bromine was destroyed with saturated sodium hydrogensulfite solution. The precipitated solid was filtered over flash silica gel with DCM. The solid was dissolved in DCM, precipitated with *iso*propanol, and dried. Dithienopyrazine **15** (720 mg, 1.44 mmol, 92%) was obtained as colorless solid. Mp 270.9-271.4 °C. ^{13}C-NMR

(125 MHz, $C_2D_2Cl_4$): δ 152.3, 145.5, 121.9, 112.4 ppm. HRMS (APCI): m/z calcd for $C_8Br_4N_2S_2+H^+$: 504.6309 $[M+H]^+$; found: 504.6311 (δm/m = 0.36 ppm).

*2,6-Dibromodithieno[2,3-b:3',2'-e]pyrazine **18***. Dithienopyrazin **6** (47 mg, 0.2 mmol) was dissolved in abs THF (0.75 mL) and cooled to -78 °C. Subsequently, phenyl lithium dissolved in dibutyl ether (0.38 mL, 1.9 mol/L, 0.73 mmol) was added and the reaction mixture kept at -78 °C for 45 min. After cooling to -95 °C, abs THF (1 mL) and tetrabromomethane (260 mg, 0.78 mmol) dissolved in abs THF (1 mL) were added at once, the reaction mixture stirred for 2 hr at -78 °C, warmed to r.t., and filtered. The obtained residue was washed with DCM, the filtrate concentrated, and purified by column chromatography (flash silica gel, DCM). Dithienopyrazine **18** (70 mg, 0.2 mmol, 82%) was obtained as colorless solid. Mp 245.3-246.9 °C. ^{1}H-NMR (400 MHz, $CDCl_3$): δ δ 7.59 ppm (s, 2H, *H*-3); ^{13}C-NMR (125 MHz, $CDCl_3$): δ 153.1, 148.1, 125.3, 122.8 ppm. HRMS (APCI): m/z calcd for $C_8H_2Br_2N_2S_2+H^+$: 348.8099 $[M+H]^+$; found: 348.8101 (δm/m = 0.51 ppm).

*2,6-Diiododithieno[2,3-b:3',2'-e]pyrazine **19***. Dithienopyrazine **6** (0.10 g, 0.52 mmol) was dissolved in abs THF (1.5 mL) and cooled to -78 °C. Subsequently, phenyl lithium dissolved in dibutyl ether (1.09 mL, 1.9 mol/L, 2.08 mmol) was added and the reaction mixture kept at -78 °C for 30 min. Then, a solution of elemental iodine (528 mg, 2.08 mmol) in abs THF (1.5 mL) was added to the reaction mixture, warmed to r.t., and stirred for 1 hr. The solvents were removed and the obtained residue purified by column chromatography (flash silica gel, PE/DCM 1:1). Dithienopyrazine **19** (190 mg, 0.43 mmol, 82%) was obtained as colorless solid. Mp 305.7-306.1 °C. ^{1}H-NMR (500 MHz, $C_2D_2Cl_4$, 80°C): δ 7.81 ppm (s, 2H, *H*-3); ^{13}C-NMR (125 MHz, $C_2D_2Cl_4$, 80°C): δ 156.1, 148.5, 132.6, 86.3 ppm. HRMS (APCI): m/z calcd for $C_8H_2I_2N_2S_2$: 443.7743 $[M]^+$; found: 443.7748 (δm/m = 0.92 ppm).

*2,6-Bis(tributylstannyl)dithieno[2,3-b:3',2'-e]pyrazine **20***. Dithienopyrazine **6** (100 mg, 0.52 mmol) was dissolved in abs THF (1.5 mL) and cooled to -78 °C. Subsequently, phenyl lithium dissolved in dibutyl ether (1.09 mL, 1.9 mol/L, 2.1 mmol) was added and the reaction mixture kept at -78 °C for 45 min. Then, a solution of tributyltin chloride (0.69 g, 0.58 mL, 2.13 mmol) in abs THF (1.5 mL) was added to the reaction mixture, warmed to r.t., and stirred for 1 hr. The solvents were removed and the obtained residue purified by column chromatography (flash silica gel, PE/DCM 3:1). Dithienopyrazine **20** (317 mg, 0.41 mmol, 80%) was obtained as colorless oil. ^{1}H-NMR (400 MHz, $CDCl_3$): δ 7.60 (s, 2H, *H*-3), 1.81-1.51 (m, 12H, α-C*H*$_2$), 1.45-1.29 (m, 12H, β-C*H*$_2$), 1.30-1.13 (m, 12H, γ-C*H*$_2$), 0.90 ppm (t, $^3J_{HH}$ = 7,3 Hz, 18H, C*H*$_3$); ^{13}C-NMR (125 MHz, $CDCl_3$): δ 155.3, 148.0, 147.95, 130.7, 29.1, 27.4, 13.8, 11.1 ppm. HRMS (ESI): m/z calcd for $C_{32}H_{56}N_2S_2Sn_2+H^+$: 763.2021 $[M+H]^+$; found: 763.2012 (δm/m = 1.21 ppm).

*3,7-Dibromodithieno[2,3-b:2',3'-e]pyrazine **16***. Dithienopyrazine **5** (0.20 g, 1.04 mmol) was suspended in chlorofomr (8 mL) and hydrobromic acid (32-% in acetic acid, 5 mL) and elemental bromine (0.2 mL, 4.16 mmol) were added. The reaction mixture was heated for 7 d at 70 °C. After cooling, saturated sodium hydrogensulfite solution was added and the obtained residue was filtered. Chloroform was evaporated from the mother liquor and the precipitated solid was filtered. The combined and dried solid was purified by column chromatography (flash silica gel, PE/ DCM 1:1) and dithienopyrazine **16** (320 mg, 0.91 mmol, 88%) was obtained as a colorless solid. Mp 290.1-291.3 °C. ^{1}H-NMR (500 MHz, $C_2D_2Cl_4$, 80°C): δ 7.94 ppm (s, 2H, *H*-2); ^{13}C-NMR (125 MHz, $C_2D_2Cl_4$, 80°C): δ 151.6, 145.0, 129.4, 108.3 ppm. HRMS (APCI): m/z calcd for $C_8H2Br_2N_2S_2+H^+$: 348.8099 $[M+H]^+$; found: 348.8105 (δm/m = 1.75 ppm).

*2,3,6,7-Tetrabromodithieno[2,3-b:2',3'-e]pyrazine **17***. Elemental bromine (16.0 mL, 312 mmol) was slowly added to the furnished solids dithienopyrazine **5** (200 mg, 1.04 mmol) and aluminum trichloride (1.39 g, 10.4 mmol) and heated for 3 d at 70 °C. After cooling, excessive bromine was destroyed with saturated sodium hydrogensulfite solution. The precipitated solid was filtered over flash silica gel with DCM. Dithienopyrazine **17** (400 mg, 0.79 mmol) was obtained as a colorless solid. Mp 312.6-313.0 °C. ^{13}C-NMR (125 MHz, $C_2D_2Cl_4$, 80°C): δ = 153.8, 144.0, 122.7, 111.1 ppm. HRMS (APCI): m/z calcd for $C_8Br_4N_2S_2+H^+$: 504.6309 $[M+H]^+$; found: 504.6328 (δm/m = 3.66 ppm).

*2,6-Dibromodithieno[2,3-b:2',3'-e]pyrazine **21***. Dithienopyrazine **5** (0.20 g, 1.04 mmol) was dissolved in abs THF (7 mL) and cooled to -78 °C. Subsequently, phenyl lithium dissolved in dibutyl ether (2.0 mL, 1.9 mol/L, 0.7 mmol) was added and the

reaction mixture kept at -78 °C for 1 hr. After cooling to -90 °C, tetrabromomethane (1.38 g, 4.16 mmol) dissolved in abs THF (7 mL) was added at once, the reaction mixture stirred for additional 10 min at -78 °C, warmed to r.t., concentrated to dryness, and purified by column chromatography (flash silica gel, DCM). Dithienopyrazine **21** (137 mg, 0.39 mmol, 38%) was obtained as a colorless solid. Mp 295.0-296.2 °C. ^{1}H-NMR (500 MHz, $C_2D_2Cl_4$, 80°C): δ 7.52 ppm (s, 2H, *H*-3); ^{13}C-NMR (125 MHz, $C_2D_2Cl_4$, 80°C): δ = 155.2, 146.3, 124.9, 122.9 ppm. HRMS (APCI): m/z calcd for $C_8H_2Br_2N_2S_2$+H$^+$: 348.8099 [M+H]$^+$; found: 348.8109 (δm/m = 2.84 ppm).

1,1'-[2,6-Bis(triisopropylsilyl)dithieno[2,3-b:3',2'-e]pyrazine-4,8-diyl]bis(ethan-1-one) ***22***. TIPS-protected dithienopyrazine **10** (500 mg, 0.99 mmol), elemental zinc powder (149 mg, 2.28 mmol), and acetic anhydride (1.9 mL, 20 mmol) were heated for 5 d at 140 °C under argon. Then, acetic anhydride was removed and methanol given to the residue. The obtained suspension was filtered and the obtained solid discarded. The filtrate was concentrated and the obtained solid dissolved in DCM and precipitated with PE. Acylated dihydropyrazine **22** (584 mg, 0.99 mmol, 99%) was obtained as a colorless solid. Mp 183.4-185.9 °C. ^{1}H-NMR (500 MHz, $C_2D_2Cl_4$, 70°C): δ 7.14 (s, 2H, *H*-3), 2.58 (s, 3H, 8-C*H*$_3$), 2.30 (s, 3H, 4-C*H*$_3$), 1.38-1.19 (m, 6H, Si(C*H*-(C*H*$_3$)$_2$)$_3$), 1.10 ppm (d, $^3J_{HH}$ = 7,3 Hz, 36H, Si-(CH)$_3$-(C*H*$_3$)$_6$); ^{13}C-NMR (125 MHz, $C_2D_2Cl_4$, 70°C): δ 167.4, 165.9, 136.4, 129.2, 23.6, 23.4, 18.9, 12.0 ppm. HRMS (MALDI-FTICR): m/z calcd for $C_{30}H_{50}N_2O_2S_2Si_2$: 590.2847 [M]$^+$; 590.2845 found: (δm/m =0.25 ppm).

1,1'-(Dithieno[2,3-b:3',2'-e]pyrazine-4,8-diyl)bis-(ethan-1-one) ***23***. Dithienopyrazine **6** (0.20 g, 1.04 mmol), elemental zinc (156 mg, 2.39 mmol), and acetic anhydride (3.0 mL, 31 mmol) were heated for 5 d at 140 °C under argon. Then, acetic anhydride was removed and methanol given to the residue. The obtained suspension was filtered, washed with DCM, and the obtained solid discarded. The filtrate was concentrated and the obtained solid purified by column chromatography (flash silica gel, DCM). Acylated dihydropyrazine **23** (270 mg, 0.97 mmol, 93%) was obtained as a colorless solid. Mp 179.8-181.8 °C. ^{1}H-NMR (500 MHz, $C_2D_2Cl_4$, 70°C): δ 7.02 (d, $^3J_{HH}$ = 5,8 Hz, 2H, *H*-2), 7.00 (d, $^3J_{HH}$ = 5,8 Hz, 2H, *H*-3), 2.56 (s, 3H, 8-C*H*$_3$), 2.31 ppm (s, 3H, 4-C*H*$_3$); ^{13}C-NMR (125 MHz, $C_2D_2Cl_4$, 70°C): δ 167.4, 166.0, 132.0, 120.7, 23.3, 23.2 ppm. (2 signals don't appear due to the coalescence temperature). HRMS (ESI): m/z calcd for $C_{12}H_{10}N_2O_2S_2$+H$^+$: 279.0257 [M+H]$^+$; found: 279.0250 (δm/m = 2.33 ppm), 316.9808 [M+K]$^+$.

1,1'-(2,6-Dibromodithieno[2,3-b:3',2'-e]pyrazine-4,8-diyl)bis(ethan-1-one) ***24***. To a solution of acylated dihydropyrazine **19** (60.0 mg, 0.22 mmol) in DCM (10 mL) *N*-bromosuccinimide (79.0 mg, 0.44mmol) was added and the reaction mixture stirred for 18 hr at r.t. The solvent was removed and the obtained residue purified by column chromatography (flash silica gel, DCM). Dihydropyrazine **24** (50.0 mg, 0.11 mmol, 53%) was obtained as a colorless solid. Mp 167.3-169.6 °C. ^{1}H-NMR (500 MHz, [D$_8$]THF, 60°C): δ = 7.22 (s, 2H, *H*-3), 2.50 (s, 3H, 8-CH$_3$), 2.28 ppm (s, 3H, 4-CH$_3$). ^{13}C-NMR (125 MHz, THF-d$_8$): δ 167.5, 166.1, 149.4, 126.8, 126.4, 123.5, 23.0, 22.6 ppm. HRMS (ESI): m/z calcd for $C_{12}H_8Br_2N_2O_2S_2$+K$^+$: 472.8026 [M+K]$^+$; found: 472.8027 (δm/ m = 0,30 ppm). As a side product, deacylated dibromopyrazine **18** (20.0 mg, 0.06 mmol, 27%) was isolated.

Oxidation of dithieno[2,3-b:3',2'-e]pyrazine ***6*** *in acetic acid.* Dithienopyrazine **6** (50.0 mg, 0.30 mmol) was dissolved in acetic acid (2 mL) and a solution of hydrogen peroxide (33% in water, 2.4 mL, 26 mmol) was added. The reaction mixture was heated for 2 d at 60 °C and after purification by column chromatography (flash silica gel, DCM) pyrazine-4-oxide **25** (12 mg, 0.06 mmol, 22%), pyrazine-1,1-dioxide **26** (10 mg, 0.04 mmol, 17%), and pyrazine-4-oxid-1,1-dioxide **27** (6 mg, 0.02 mmol, 10%) were isolated.

Analytical data of **25**: Mp 218.5-219.3 °C. IR: 1243 cm^{-1}. ^{1}H-NMR (400 MHz, $CDCl_3$): δ 7.80 (d, $^3J_{HH}$ = 6,3 Hz, 2H, *H*-2), 7.70 ppm (d, $^3J_{HH}$ = 6,3 Hz, 2H, *H*-3); ^{13}C-NMR (100 MHz, CD_2Cl_2): δ 156.0, 137.4, 129.3, 115.9 ppm. IR: 529, 697, 749, 770, 823, 835, 1007, 1027, 1072, 1089, 1216, 1243, 1338, 1418, 1517, 2851, 2921, 3065, 3106 cm^{-1}. HRMS (ESI): m/z calcd for $C_8H_4N_2OS_2$+H$^+$: 208.9838 [M+H]$^+$; found: 208.9841 (δm/m = 1.39 ppm), 438.9433 [2M+Na]$^+$.

Analytical data of **26**: Mp 207.2-208.1 °C. IR: 1161, 1311 cm^{-1}. ^{1}H-NMR (400 MHz, $CDCl_3$): δ 7.91 (d, $^3J_{HH}$ = 6.2 Hz, 1H, *H*-6), 7.85 (d, $^3J_{HH}$ = 7.9 Hz, 1H, *H*-2), 7.78 (d, $^3J_{HH}$ = 6.2 Hz, 1H, *H*-5), 7.00 ppm (d, $^3J_{HH}$ = 7.9 Hz, 1H, *H*-3). IR: 426, 492, 591, 710, 805, 821, 852, 1007, 1058, 1123, 1161, 1214, 1247, 1311, 1465, 1410, 3038,

3104, 3114 cm^{-1}. HRMS (ESI): m/z calcd for $C_8H_4N_2O_2S_2+H^+$: 224.9787 $[M+H]^+$; found: 224.9787 (δm/m = 0.09 ppm), 470.93232 $[2M+Na]^+$. A ^{13}C NMR spectrum was not possible due to the low solubility in various organic solvents.

Analytical data of **27**: Mp 212.3-213.1 °C. IR: 1163, 1315 cm^{-1}. ^1H-NMR (400 MHz, $CDCl_3$): δ 8.16 (d, $^3J_{HH}$ = 6.1 Hz, 1H, *H*-6), 7.62 (d, $^3J_{HH}$ = 6.1 Hz, 1H, *H*-5), 7.51 (d, $^3J_{HH}$ = 7.8 Hz, 1H, *H*-2), 7.14 ppm (d, $^3J_{HH}$ = 7.8 Hz, 1H, *H*-3). IR: 428, 498, 547, 574, 593, 657, 679, 693, 753, 794, 1023, 1066, 1080, 1124, 1163, 1235, 1260, 1315, 1464, 1529, 1739, 2851, 2921, 3069 cm^{-1}. HRMS (ESI): m/z calcd for $C_8H_4N_2O_3S_2$: 240.9736 $[M+H]^+$; found: 240.9737 (δm/m = 0.45 ppm), 480.9407 $[2M+H]^+$. A ^{13}C NMR spectrum was not possible due to the low solubility in various organic solvents.

*Oxidation of dithieno[2,3-b:3',2'-e]pyrazine **6** in trifluoroacetic acid.* Dithienopyrazine **6** (50.0 mg, 0.30 mmol) was dissolved in trifluoroacetic acid (1 mL) and a solution of hydrogen peroxide (33% in water, 1.0 mL, 12 mmol) was added. The reaction mixture was heated for 2 hr at 100 °C and after purification by column chromatography (flash silica gel, DCM/EA 9:1) pyrazine-4-oxid-1,1-dioxide **27** (10 mg, 0.04 mmol, 16%) and pyrazine-4,8-dioxid-1,1-dioxide **28** (5 mg, 0.02 mg, 8%) were isolated.

Analytical data of **28**: Mp 210.9-211.3 °C. IR: 1155, 1260, 1325 cm^{-1}. ^1H-NMR (400 MHz, $CDCl_3$): δ 7.84 (d, $^3J_{HH}$ = 5.9 Hz, 1H, *H*-6), 7.77 (d, $^3J_{HH}$ = 5.9 Hz, 1H, *H*-5), 7.74 (d, $^3J_{HH}$ = 7.7 Hz, 1H, *H*-2), 6.96 ppm (d, $^3J_{HH}$ = 7.7 Hz, 1H, *H*-3). IR: 551, 700, 739, 801,969, 1012, 1078, 1155, 1181, 1241, 1260, 1325, 1370, 1463, 1570, 1733, 2853, 2923, 2954 cm^{-1}. HRMS (ESI): m/z calcd for $C_8H_4N_2O_4S_2+Na^+$: 278.9505 $[M+Na]^+$; found: 278.9511 (δm/m = 2.40 ppm), 534.9145 $[2M+Na]^+$. A ^{13}C NMR spectrum was not possible due to the low solubility in various organic solvents. The analytical data of dioxide **27** were identical to the data described above.

*3,5-Bis[5-(trimethylsilyl)thien-2-yl]-dithieno[2,3-b:3',2'-e]pyrazine **30***. 3,5-Dibromo-dithienopyrazine **14** (100 mg, 0.29 mmol), trimethyl[5-(4,4,5,5-tetramethyl-1,3,2-dioxaborolan-2-yl)thien-2-yl]silane **29** (177 mg, 0.63 mmol), Pd_2dba_3 (26.0 mg, 0.03 mmol, 10 mol%) and $HP(t\text{-}Bu)_3BF_4$ (17.0 mg, 0.06 mmol, 20 mol%) were suspended in abs THF (5 mL) and degassed with argon for 30 min. Then, a degassed solution of potassium carbonate (237 mg, 1.71 mmol) in demineralized water (5 mL) was added and the reaction mixture stirred for 15 hr at r.t. The reaction mixture was poured into water and extracted three times with DCM. The combined organic phases were concentrated and purified by column chromatography (flash silica gel, PE/DCM 2:1). Dithienopyrazine **30** (105 mg, 0,21 mmol, 73%) was obtained as a yellow solid. Mp 153.5-156.5 °C. ^1H-NMR (400 MHz, $CDCl_3$): δ 8.25 (d, $^3J_{HH}$ = 3.5 Hz, 2H, *H*-3‘), 8.01 (s, 2H, *H*-2), 7.34 (d, $^3J_{HH}$ = 3.5 Hz, 2H, *H*-4‘), 0.42 ppm (s, 18H, $Si(CH_3)_3$). ^{13}C-NMR (100 MHz, $CDCl_3$): δ = 152.9, 144.2, 140.5, 140.5, 134.6, 128.6, 127.2, 125.2, 0.1 ppm. HRMS (MALDI-FTICR): m/z calcd for $C_{22}H_{24}N_2S_4Si_2$: 500.0355 [M]+; found: 500.0355 (δm/m = 0.16 ppm).

*2,3,5,6-Tetrakis[5-(trimethylsilyl)thien-2-yl]dithieno[2,3-b:3',2'-e]pyrazine **31***. Tetrabromopyrazine **15** (50.0 mg, 0.10 mmol) and trimethyl[5-(4,4,5,5-tetramethyl-1,3,2-dioxaborolan-2-yl)thien-2-yl]silane **29** (167 mg, 0.59 mmol) were suspended in a solvent mixture of THF (2.5 mL) and water (2.5 mL) and degassed with argon for 1 hr. Then, Pd_2dba_3 (9.0 mg, 0.01 mmol, 10 mol%), $HP(t\text{-}Bu)_3BF_4$ (6.0 mg, 0.02 mmol, 20 mol%) and potassium carbonate (81 mg, 0.59 mmol) were added and the reaction mixture heated for 22 hr at 60 °C. The reaction mixture was poured into water and extracted three times with DCM. The combined organic phases were concentrated and purified by column chromatography (flash silica gel, PE/DCM 3:1). Dithienopyrazine **31** (50.0 mg, 0.06 mmol, 63%) was isolated as yellow solid. Mp 191.9-193.4 °C. ^1H-NMR (400 MHz, $CDCl_3$): δ 7.65 (d, $^3J_{HH}$ = 3.5 Hz, 2H, *H*-3‘ or *H*-3‘‘), 7.41 (d, $^3J_{HH}$ = 3.5 Hz, 2H, *H*-3‘ or *H*-3‘‘), 7.24 (d, $^3J_{HH}$ = 3.5 Hz, 2H, *H*-4‘ or *H*-4‘‘), 7.21 (d, $^3J_{HH}$ = 3.5 Hz, 2H, *H*-4‘ or *H*-4‘‘), 0.35 (s, 18H, Si-$(CH_3)_3$), 0.35 (s, 18H, Si-$(CH_3)_3$); ^{13}C-NMR (100 MHz, $CDCl_3$): δ 151.7, 147.3, 145.0, 142.1, 140.1, 138.5, 136.4, 134.5, 133.8, 130.4, 130.4, 124.7, 0.2, 0.0 ppm. HRMS (MALDI-FTICR): m/z calcd for $C_{36}H_{44}N_2S_6Si_4$: 808.0900 [M]+; found: 808.0900 (δm/m = 0.01ppm).

*2,6-Bis[5-(trimethylsilyl)thien-2-yl]dithieno[2,3-b:3',2'-e]pyrazine **32***. Dibromodithienopyrazine **18** (100 mg, 0.29 mmol), trimethyl[5-(4,4,5,5-tetramethyl-1,3,2-dioxaborolan-2-yl)thien-2-yl]silane **29** (177 mg, 0.63 mmol), Pd_2dba_3 (26.0 mg, 0.03 mmol, 10 mol%) and $HP(t\text{-}Bu)_3BF_4$ (17.0 mg, 0.06 mmol, 20 mol%) were suspended in abs THF

(5 mL) and degassed with argon for 30 min. Then, a degassed solution of potassium carbonate (237 mg, 1.71 mmol) in demineralized water (5 mL) was added and the reaction mixture stirred for 15 hr at r.t. The reaction mixture was poured into water and extracted three times with DCM. The combined organic phases were concentrated and purified by column chromatography (flash silica gel, PE/DCM 2:1). Dithienopyrazine **32** (100 mg, 0.21 mmol, 70%) was obtained as a yellow solid. Mp 208.0-209.1 °C. ^{1}H-NMR (400 MHz, $CDCl_3$): δ 7.46 (s, 2H, *H*-3), 7.42 (d, $^3J_{HH}$ = 3.5 Hz, 2H, *H*-3‘), 7.19 (d, $^3J_{HH}$ = 3,5 Hz, 2H, *H*-4‘), 0.37 ppm (s, 18H, Si(C*H*$_3$)$_3$); ^{13}C-NMR (100 MHz, $CDCl_3$): δ = 151.76, 149.02, 143.94, 141.57, 141.38, 135.08, 127.56, 117.06, -0.05 ppm. HRMS (MALDI-FTICR): m/z calcd for $C_{22}H_{24}N_2S_4Si_2$: 500.0355 [M]+; found: 500.0353 (δm/m = 0.42 ppm).

*3,5-Bis[(trimethylsilyl)ethynyl]dithieno[2,3-b:3',2'-e]pyrazine **34***. Dibrominated dithienopyrazine **14** (40.0 mg, 0.11 mmol) was dissolved in abs toluene (5 mL), which was degassed with argon. Subsequently, triethylamine (2.5 mL), $Pd(PPh_3)_2Cl_2$ (8.0 mg, 0.01 mmol, 9 mol%), copper iodide (0.4 mg, 2.1 µmol, 2 mol%), and trimethylsilylacetylene **33** (0.06 mL, 0.46 mmol) were added and the reaction mixture stirred for 48 hr at 50 °C. After cooling, the solvents were removed and the obtained residue purified by column chromatography (flash silica gel, PE/DCM 1:1). Dithienopyrazine **34** (30.0 mg, 0.08 mmol, 68%) was obtained as a yellow resin. ^{1}H-NMR (400 MHz, $CDCl_3$): δ 8,09 (s, 2H, *H*-2), 0,33 ppm (s, 18H, Si(C*H*$_3$)$_3$); ^{13}C-NMR (100 MHz, $CDCl_3$): δ 151,7, 146,8, 135,5, 118,0, 99,6, 96,4, 0,1 ppm. HRMS (ESI): m/z calcd for $C_{18}H_{20}N_2S_2Si_2$+H^+: 385.0679 [M+H]$^+$; found: 385.06700 (δm/m = 2.41 ppm).

*2,3,5,6-Tetrakis[(trimethylsilyl)ethynyl]dithieno[2,3-b:3',2'-e]pyrazine **35***. A suspension of tetrabromodithienopyrazine **15** (50.0 mg, 0.1 mmol), $Pd(PPh_3)_2Cl_2$ (7.0 mg, 0.01 mmol, 10 mol%), copper iodide (0.4 mg, 2.1 µmol, 2 mol%) and abs toluene (4 mL) was degassed with argon for 1 hr. Then, triethylamine (2 mL), and trimethylsilylacetylene **33** (0.2 mL, 1.46 mmol) were added and the reaction mixture stirred for 24 hr at 110 °C. After cooling, the solvents were removed and the obtained residue purified by column chromatography (flash silica gel, PE). Dithienopyrazine **35** (40.0 mg, 0.07 mmol, 70%) was obtained as a light yellow resin. ^{1}H-NMR (400 MHz, $CDCl_3$): δ 0,34 (s, 18H, Si(C*H*$_3$)$_3$), 0,33 ppm (s, 18H, Si(C*H*$_3$)$_3$); ^{13}C-NMR (100 MHz, $CDCl_3$): δ 152,2, 146,9, 131,0, 122,4, 111,7, 104,7, 96,4, 95,7, 0,1, -0,2 ppm. HRMS (ESI): m/z calcd for $C_{28}H_{36}N_2S_2Si_4$+H^+: 577.1470 [M+H]$^+$; found: 577.1520 (δm/m = 0.05 ppm).

*2,6-Bis[(trimethylsilyl)ethynyl]dithieno[2,3-b:3',2'-e]pyrazin **36***. Dibrominated dithienopyrazine **18** (70 mg, 0.2 mmol) was dissolved in abs toluene (15 mL) and degassed with argon for 30 min. Then, $Pd(PPh_3)_2Cl_2$ (14.0 mg, 0.02 mmol, 10 mol%), copper iodide (0.7 mg, 3.1 µmol, 1.5 mol%), trimethylsilylacetylene **33** (0.06 mL, 0.40 mmol), and triethylamine (5 mL) were added and the reaction mixture stirred for 24 hr at r.t. The reaction solution was concentrated and purified by column chromatography (flash silica gel, PE/DCM 1:1). Dithienopyrazine **36** (76 mg, 0.2 mmol, 98%) was isolated as a colorless solid. Mp 188.5-189.8 °C. ^{1}H-NMR (400 MHz, $CDCl_3$): δ 7,59 (s, 2H, *H*-3), 0,31 ppm (s, 18H, Si(C*H*$_3$)$_3$); ^{13}C-NMR (100 MHz, $CDCl_3$): δ = 153,4, 147,9, 128,3, 127,1, 106,7, 96,9, -0,2 ppm. HRMS (ESI): m/z calcd for $C_{18}H_{20}N_2S_2Si_2$+H^+: 385.0679 [M+H]$^+$; found: 385.0670 (δm/m = 2.39 ppm).

Keywords
Dithienopyrazine, electrophilic halogenation, lithiation, C-C coupling reaction, X-ray structure analysis.

Author Information
Corresponding author
Peter Bäuerle – ORCID 0000-0003-2017-4414
E-mail: peter.baeuerle@uni-ulm.de
Coauthor
Elena Mena-Osteritz – ORCID 0000-0002-4639-1823; E-mail: elena.mena-osteritz@uni-ulm.de

References

[1] S. R. Forrest, Organic Electronics: Foundation to Applications, Oxford University Press, **2020**.
[2] J. E. Anthony, *Chem. Rev.* **2006**, *106*, 5028–5048.
[3] Y. Shimo, T. Mikami, S. Hamao, H. Goto, H. Okamoto, R. Eguchi, S. Gohda, Y. Hayashi, Y. Kubozono, *Sci. Rep.* **2016**, *6*, 1–13.
[4] A. Narita, X.-Y. Wang, X. Feng, K. Müllen, *Chem. Soc. Rev.* **2015**, *44*, 6616–6643.
[5] U. H. F. Bunz, J. U. Engelhart, B. D. Lindner, M. Schaffroth, *Angew. Chem.* **2013**, 125, 3898–3910, *Angew. Chem. Int. Ed.* **2013**, *52*, 3810–3821.
[6] F. Ding, D. Xia, W. Sun, W. Chen, Y. Yang, K. Lin, F. Zhang, X. Guo, *Chem. Eur. J.* **2019**, *25*, 15106–15111.

[7] W. Ye, Y. Yang, Z. Zhang, Y. Zhu, L. Ye, C. Miao, Y. Lin, S. Zhang, *Sol. RRL* **2020**, *4*, 2000258.
[8] H. Yao, L. Ye, H. Zhang, S. Li, S. Zhang, J. Hou, *Chem. Rev.* **2016**, *116*, 7397–7457.
[9] S. Alem, S. Wakim, J. Lu, G. Robertson, J. Ding, Y. Tao, *ACS Appl. Mater. Interfaces* **2012**, *4*, 2993–2998.
[10] Q. Miao, *Synlett* **2012**, *23*, 326–336.
[11] Z. Zhang, Y.-S. Wu, K.-C. Tang, C. L. Chen, J. W. Ho, J. Su, H. Tian, P. T. Chou, *J. Am. Chem. Soc.* **2015**, *137*, 8509–8520.
[12] U. H. F. Bunz, *Chem. Eur. J.* **2009**, *15*, 6780–6789.
[13] Z. Liang, Q. Tang, R. Mao, D. Liu, J. Xu, Q. Miao, *Adv. Mater.* **2011**, *23*, 5514–5518.
[14] X. Chen, J. Guo, L. Zou, A. Ren, J. Fan, *J. Phys. Chem. C* **2011**, *115*, 21416–21428.
[15] Z. Liang, Q. Tang, J. Xu, Q. Miao, *Adv. Mater.* **2011**, *23*, 1535–1539.
[16] Y. Liu, C. Song, W. Zeng, K. Zhou, Z. Shi, C. Ma, *J. Am. Chem. Soc.* **2010**, *132*, 16349–16351.
[17] N. Hayashi, N. Okamoto, N. Sasaki, M. Ito, J. Yoshino, H. Higuchi, *Heterocycles* **2015**, *93*, 250–258.
[18] https://goldbook.iupac.org/terms/view/ A00381, accessed: 13.12.2022.
[19] D. S. Rao, B. D. Tilak, *J. Sci. Ind. Res.* **1957**, *16 B*, 65–68.
[20] D. S. Rao, B. D. Tilak, *J. Sci. Ind. Res.* **1954**, *13 B*, 829–833.
[21] N. Aggarwal, D. W. H. MacDowell, *Org. Prep. Proced. Int.* **1979**, *11*, 247–249.
[22] K. Takimiya, Y. Konda, H. Ebata, N. Niihara, T. Otsubo, *J. Org. Chem.* **2005**, *70*, 10569–10571.
[23] T. Kashiki, S. Shinamura, M. Kohara, E. Miyazaki, K. Takimiya, M. Ikeda, H. Kuwabara, *Org. Lett.* **2009**, *11*, 2473–2475.
[24] H. Wynberg, J. De Wit, H. J. Sinnige, *J. Org. Chem.* **1970**, *35*, 711–715.
[25] M. P. Boone, Y. Dienes, T. Baumgartner, *ARKIVOC* **2009**, *5*, 90–101.
[26] C. Peinador, M. C. Veiga, J. Vilar, J. M. Quintela, *Heterocycles* **1994**, *38*, 1299–1305.
[27] J. M. Quintela, C. Peinador, M. C. Veiga, L. M. Botana, A. Alfonso, R. Riguera, *Eur. J. Med. Chem.* **1998**, *33*, 887–897.
[28] D. V Vilarelle, C. Peinador, J. M. Q. Lopez, *Tetrahedron* **2004**, *60*, 275–283.
[29] G. Seitz, J. Richter, *Chem. Ber.* **1989**, *122*, 2177–2181.
[30] A. W. Erian, F. A. Abu-Shanab, *Bull. Chem. Soc. Jpn.* **1998**, *71*, 2387–2391.
[31] J. Zhang, J. Wang, X. Xu, S. Chen, Q. Zhang, C. Yao, X. Zhuang, A. Pan, L. Li, *J. Mater. Chem. C* **2015**, *3*, 5933–5939.
[32] F. Outurquin, C. Paulmier, *Tetrahedron Lett.* **1993**, *34*, 5719–5722.
[33] P. Oechsle, P. Hou, U. Flörke, J. Paradies, *Adv. Synth. Catal.* **2016**, *358*, 3770–3776.
[34] T. Hosoya, R. Iimori, S. Yoshida, Y. Sumida, Y. Sahara-Miura, J. Sato, S. Inouye, *Org. Lett.* **2015**, *17*, 3888–3891.
[35] J. E. Baldwin, *J. Chem. Soc., Chem. Commun.* **1976**, 734–736.
[36] F. Kreuzer, PhD thesis, University of Ulm, 2020.
[37] P. Meti, E.-S. Lee, J.-W. Yang, Y.-D. Gong, *RSC Adv.* **2017**, *7*, 18120–18131
[38] W. L. Neumann, R. Rajagopalan, R. B. Dorshow, Patent WO2007149478A2, **2007**.
[39] S. W. Schneller, F. W. Clough, L. E. Hardee, *J. Heterocycl. Chem.* **1976**, *13*, 273–275.
[40] E. C. Taylor, J. E. Macor, *J. Org. Chem.* **1987**, *52*, 4280–4287.
[41] H. Sashida, K. Sadamori, T. Tsuchiya, *Synth. Commun.* **1998**, *28*, 713–727.
[42] S. H. Jang, T. B. Tai, M. K. Kim, J. W. Han, Y. Kim, S. C. Shin, Y. J. Yoon, S. K. Kwon, S.-G. Lee, *Bull. Korean Chem. Soc.* **2009**, *30*, 618–622.
[43] H. Pan, Y. Li, Y. Wu, P. Liu, S. Ong, S. Zhu, G. Xu, *J. Am. Chem. Soc.* **2007**, *129*, 4112–4113.
[44] S. Jiang, Y. Ma, Y. Wang, C. Wang, Y. Shen, *Chin. J. Chem.* **2014**, *32*, 298–306.
[45] D. Wei, K. Xie, H. Ding, Z. Chen, Patent CN 109836436 A 20190604, **2019.**
[46] D. N. D'Aleo, S. R. Allard, C. C. Foglia, S. L. M. Parent, D. J. Rohr, C. Gottardo, C. D. MacKinnon, *Can. J. Chem.* **2013**, *91*, 679–683.
[47] H. Chen, M. Nikolka, A. Wadsworth, W. Yue, A. Onwubiko, M. Xiao, A. J. P. White, D. Baran, H. Sirringhaus, I. Mcculloch, *Macromolecules* **2018**, *51*, 71–79.
[48] L. H. Klemm, J. N. Louris, *J. Heterocycl. Chem.* **1984**, *21*, 785–789.
[49] R. Rieger, D. Beckmann, A. Mavrinskiy, M. Kastler, M. Klaus, *Chem. Mater.* **2010**, 5314–5318.
[50] P. Sonar, J. Zhang, A. C. Grimsdale, K. Müllen, M. Surin, R. Lazzaroni, P. Leclère, S. Tierney, M. Heeney, I. McCulloch, *Macromolecules* **2004**, *37*, 709–715.
[51] J. A. Schwindeman, T. L. Rathman, *Org. Process Res. Dev.* **2014**, *18*, 1192–1210.
[52] H. J. Reich, D. P. Green, M. A. Medina, W. S. Goldenberg, B. Ö. Gudmundsson, R. R. Dykstra, N. H. Phillips, *J. Am. Chem. Soc.* **1998**, *120*, 7201–7210.
[53] M. Mikulla, *Chern. Ber.* **1994**, *127*, 1723–1728.
[54] R. Engqvist, B. Stensland, J. Bergman, *Tetrahedron* **2005**, *61*, 4495–4500.
[55] The Chemistry of Heterocyclic Compounds, Vol. 44, *Thiophene and Its Derivatives*, S. Gronowitz (ed.), Wiley Blackwell, **1985**.
[56] K. N. Brown, J. H. Espenson, *Inorg. Chem.* **1996**, *35*, 7211–7216.
[57] B. Klein, J. Berkowitz, *J. Am. Chem. Soc.* **1959**, *81*, 5160–5166.

[58] C. G. Kruse, P. B. M. W. M. Timmermans, C. van der Laken, A. van der Gen, *Rec. Trav. Chim. Pays-Bas* **1978**, *97*, 151–180.
[59] L. H. Klemm, J. T. Barnish, R. Zell, *J. Heterocycl. Chem.* **1970**, *7*, 81–89.
[60] L. H. Klemm, J. N. Louris, W. Boisvert, H. Clay, D. R. Muchiri, *J. Heterocycl. Chem.* **1985**, *22*, 1249–1252.[61] L. H. Klemm, R. E. Merrill, *J. Heterocycl. Chem.* **1972**, *9*, 293–298.
[62] L. H. Klemm, J. N. Louris, *Heterocycl. Commun.* **1996**, *2*, 493–498.
[63] A. P. Gaywood, L. Hill, S. H. Imam, H. Mcnab, *New J. Chem.* **2010**, *34*, 236–242.
[64] J. Coates, *Interpretation of Infrared Spectra - A Practical Approach*, John Wiley & Sons, New-York, **2006**.
[65] M. Hesse, H. Meier, B. Zeeh, *Spektroskopische Methoden in der Organischen Chemie*, Thieme, Stuttgart, **2005**.
[66] M. Bohle, O. Ceder, M. G. Hoffmann, M. Müller, A. Nowak, S. von Angerer, *Hetarenes IV - Six-Membered Rings and Larger Hetero-Rings with Maximum Unsaturation*, Houben-Weyl, Stuttgart, **1998**.
[67] P. J. Wheatley, *Acta Cryst*. **1957**, *10*, 182-187.
[68] R. A. Aitken, B. Fodi, M. H. Palmer, A. M. Z. Slawin, J. Yang, *Tetrahedron* **2012**, *68*, 5845–5851.
[69] CryaAlis^{Pro}, Agilent Technologies XRD Products
[70] L. Palatinus, G. Chapuis, *J. Appl. Crystallogr.* **2007**, *40*, 786-790.
[71] L. Palatinus, A. van der Lee, *J. Appl. Crystallogr.* **2008**, *41*, 975-984
[72] L. Palatinus, S. J. Prathapa, S. van Smaalen, *J. Appl. Crystallogr.* **2012**, *45*, 575-580.
[73] G. M. Sheldrick, *Acta Cryst. A* **2008**, *64*, 112-122.
[74] Y. Wang, J. Song, L. Xu, Y. Kan, J. Shi, H. Wang, *J. Org. Chem.* **2014**, *79*, 2255–2262.